09.6

Analysis of the regularities of forward four-wave mixing in a cubic photorefractive (001)-cut crystal

© V.N. Naunyka

I.P.Shamyakin Mozyr State Pedagogical University, Mozyr, Republic of Belarus
E-mail: valnav@inbox.ru

Received August 3, 2023
Revised September 7, 2023
Accepted September 7, 2023

The problem of the forward four-wave mixing on phase holographic gratings in a cubic photorefractive absorbing crystal of symmetry class 23 is considered. The dependence of the reflection coefficient on the thickness of a crystalline sample has been studied. Conditions under which the reflection coefficient value optimized in terms of the azimuth of the linear polarization of light waves reaches its highest values have been established. The effect of phase shifts between the holographic gratings and corresponding interference patterns on the intensity of the phase-conjugated wave is discussed.

Keywords: photorefractive crystal, four-wave mixing, holographic grating, reflection coefficient, diffraction efficiency.

DOI: 10.61011/TPL.2023.10.57064.19699

Photorefractive crystals (PRCs) possess a number of advantages as compared with conventional photosensitive holographic materials (for instance, bichromated gelatin, silver halide emulsions, etc.) because they enable efficient electrical control of light wave diffraction and real-time operation, and, in addition, have high performance characteristics [1]. Due to this, such crystals are in demand for creating modern information and telecommunication systems [2]. In recent years, the field of employing PRCs in biotechnological and medical applications has been significantly extended [3].

The effect of four-wave mixing (FWM) on anisotropic phase gratings in PRC is used in designing optical generators and in creating devices intended for conjugating the light beam wavefront [4]. To find orientation dependences of the reflection coefficient, the authors of early works (see, for example, [5]) considered the cases when only one holographic grating (hereinafter referred to as grating) gets formed in the crystal as a result of FWM. In the general case of a forward FWM, the maximum possible number of gratings recorded in PRC can reach six, two of which are transmission and four are reflection gratings [6]. In recent studies [7,8] it was shown that only careful consideration of the partial diffraction contributions of all the gratings forming in PRC can provide satisfactory agreement between the results of numerical simulations and available experimental data. However, in papers [7,8] the diffraction contributions of the gratings recorded in PRC were not considered separately, and the effect of phase shifts of the gratings with respect to the corresponding interference patterns on the intensity of the phase-conjugated wave was not analyzed. Solving this problem will make it possible to more accurately predict the experimental conditions under which an increase in the FWM efficiency on shifted gratings may be achieved. This was just the goal of this study.

Let us consider an (001)-cut crystal of $Bi_{12}SiO_{20}$ (BSO), to which there are directed linearly polarized pump waves 1 and 2, as well as signal wave 3, whose wave normals lie in incidence plane I and coincide in direction with unit vectors $\mathbf{e}_{1n}$, $\mathbf{e}_{2n}$ and $\mathbf{e}_{3n}$, respectively (Fig. 1). Assume that, during the waves 1, 2 and 3 mixing in PRC, three primary phase-structure gratings (one transmission and two reflection gratings) are recorded. During the diffraction of waves 1, 2 and 3 on the primary gratings there arises phase-conjugated wave 4 whose wave normal coincides in direction with unit vector $\mathbf{e}_{4n}$. Mixing of phase-conjugated wave 4 with waves 1, 2 and 3 leads to secondary recording of the transmission grating with wave vector $\mathbf{K}_{24}$ and reflection gratings with wave vectors $\mathbf{K}_{14}$ and $\mathbf{K}_{34}$.

Fig. 1 presents the orthonormal basis $(\mathbf{e}_1, \mathbf{e}_2, \mathbf{e}_3)$ where $\mathbf{e}_3 = [\mathbf{e}_1 \times \mathbf{e}_2]$ ($\mathbf{e}_3$ is not shown), which is rigidly connected to the holographic table I surface. Orientation angle θ is used to specify the crystal rotation angle relative to the 0z axis and is equal to the angular distance between ort $\mathbf{e}_1$ and unit vector $\mathbf{q}$ fixed in the crystallographic frame of reference. Orthonormal bases ($\mathbf{e}_{jp}$, $\mathbf{e}_{js}$, $\mathbf{e}_{jn}$), where $\mathbf{e}_{jn} = [\mathbf{e}_{jp} \times \mathbf{e}_{js}]$ ($j = 1, 2, 3, 4$), are used to describe the polarization state of the j-th wave. The angles between vectors $\mathbf{e}_{jn}$ and axis 0z are designated as φ_j and are equal to the Bragg angle. Light-wave electric field vectors $\mathbf{E}_j$ lie in the planes containing vectors $\mathbf{e}_{jp}$, $\mathbf{e}_{js}$ and are oriented at azimuths ψ_j relative to vectors $\mathbf{e}_{jp}$. In further calculations, azimuths ψ_j were chosen so that at each z inside the crystal ($0 < z \leqslant d$) vectors $\mathbf{E}_1$ and $\mathbf{E}_2$, as well as $\mathbf{E}_3$ and $\mathbf{E}_4$, remained parallel to each other. In addition, equality $\psi_1 = \psi_3 = \psi$ was assumed to be satisfied at $z = 0$. If these conditions are met, the initial modulation depth of the interference patterns is optimal. We

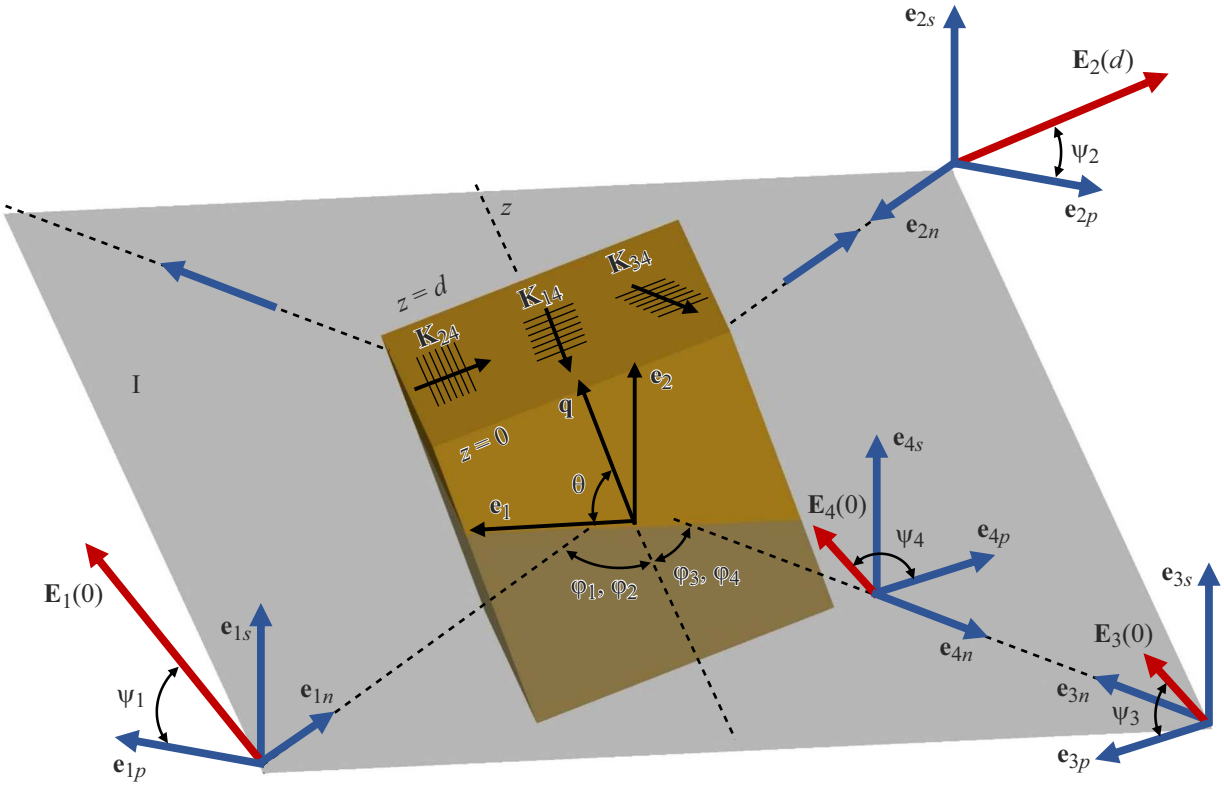

Figure 1. Schematic representation of the geometry of forward four-wave mixing in the photorefractive crystal.

assume that the PRC working faces have an antireflection coating.

The components of field strength vectors $\mathbf{E}_j$ were found by numerically solving the coupled-wave equations given in [8]. The theoretical model takes into account the linear electro-optical, photoelastic and inverse piezoelectric effects, as well as optical activity, natural absorption and circular dichroism of the crystal. The PRC physical parameters used in calculations are presented in [9]. The pump wave intensities were assumed to be equal to each other, while the ratio between intensities of the signal and pump waves was 1:20. In the calculations, angles φ_j were chosen equal to 5°. Analyzing the influence of each of the six gratings on the phase-conjugated wave characteristics is, in general, a rather cumbersome task; thus, we will restrict ourselves to considering diffraction contributions of three secondary gratings.

In Figs. 2 and 3, the solid line (curve *2*) represents the crystal-thickness dependence of diffraction efficiency η of reflection grating 14, which was obtained by numerically solving the coupled-wave equations [9] under the assumption that initial intensities of waves 2, 3 and 4 are zero. For ease of comparison, reflection coefficient R and diffraction efficiency η are expressed in relative units. The dash-and-dot lines in Figs. 2, *a* and 3 represent the thickness dependences of the highest $R^{\max}$ (curve *1*) and lowest $R^{\min}$ (curve *3*) reflection coefficients, which were found as follows. As a result of enumeration of azimuths ψ in the range from 0 to 180° with a step of 2°, a series of parameter R values was formed for each d, from which $R^{\max}$ and $R^{\min}$ were selected. In the course of constructing the dependences shown in Fig. 2, *b*, it turned out that parameter R is independent of azimuth ψ, and the curves of dependences $R^{\max}(d)$, $R^{\min}(d)$ degenerate into dependence $R(d)$ (dashed and dotted curves) calculated for various phase shifts of gratings 14 and 34 relative to the corresponding interference patterns ($\delta_{14} = \delta_{34} = \pi/2$ — curve *1*; $\delta_{14} = \pi/2$, $\delta_{34} = -\pi/2$ — curve *3*).

As shown in Figs. 2 and 3, the diffraction efficiency of reflection grating 14 does not depend on azimuth ψ. During FWM on shifted gratings 14 and 24, the wave 4 intensity becomes a function of azimuth ψ, and envelopes of maximum $R^{\max}(d)$ and minimum $R^{\min}(d)$ reflection coefficients appear. Since $R^{\max}$ exceeds diffraction efficiency η at any thickness d, we can conclude that FWM induces greater wave 4 intensities than in the case of the classical scheme of the light wave diffraction by a reflection grating. This is due to the fact that, when the optimal values of azimuth ψ are chosen, the diffraction contributions of reflection grating 14 and transmission grating 24 will be coherently summed, which will lead to an increase in the wave 4 intensity at the exit from the crystal.

As is known (see [10]), if condition $\rho d = \pi/2, 3\pi/2, \ldots$ is satisfied (where ρ is the crystal specific rotation), diffraction efficiencies of the reflection grating in the (001)-cut BSO crystal are close to zero. However, during FWM,

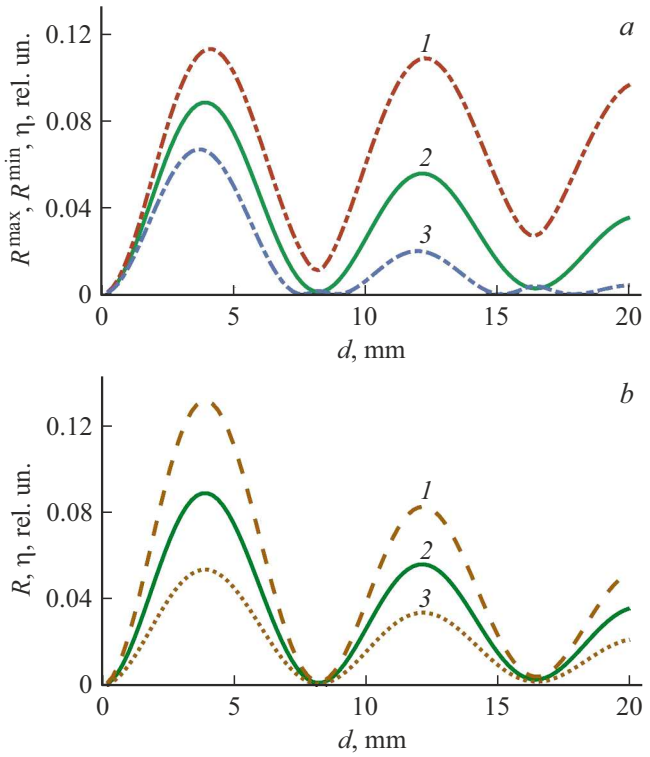

Figure 2. *a* — diffraction efficiency η of the reflection hologram (curve *2*) and reflection coefficients R^{max} (curve *1*), R^{min} (curve *3*) during FWM versus crystal thickness d. Dependences $R^{max}(d)$, $R^{min}(d)$ were calculated for the case when gratings 14 and 24 get formed during FWM in a photorefractive crystal. *b* — diffraction efficiency η of the reflection hologram (curve *2*) and reflection coefficient R (curves *1* and *3*) during FWM versus crystal thickness d. Dependences $R(d)$ were calculated for the cases when gratings 14 and 34 get formed during FWM in the photorefractive crystal with the following phase shifts: *1* — $\delta_{14} = \delta_{34} = \pi/2$; *3* — $\delta_{14} = \pi/2$, $\delta_{34} = -\pi/2$.

the phase-conjugated wave intensity for such values of d will significantly exceed the intensity of the wave reconstructed by the wave 1 diffraction on reflection grating 14 due to the constructive interference of partial diffracted waves being formed during the light waves diffraction on gratings 14 and 24. In calculating the curves presented in Fig. 2, *a*, phase shifts δ_{14} and δ_{24} were assumed to equal $\pi/2$, and change in their sign did not lead to transformation of the $R^{max}(d)$ and $R^{min}(d)$ envelopes.

In contrast to the previous case, FWM on gratings 14 and 34 makes the intensity of wave 4 practically independent of azimuth ψ (Fig. 2, *b*) and governable to a great extent by phase shifts δ_{14} and δ_{34}. If the gratings are shifted by $\pi/2$ (curve *1*), their diffraction contributions get coherently summed, and the wave 4 intensity is higher than diffraction efficiency η at any d. The opposite situation occurs if phase shifts δ_{14} and δ_{34} are equal in magnitude but different in signs ($\delta_{14} = \pi/2$, $\delta_{34} = -\pi/2$). In this case, their diffraction contributions get coherently subtracted, and condition $R \leqslant \eta$ is satisfied at any d.

For FWM on gratings 14, 24 and 34, Fig. 3, *a* presents dependences $R^{max}(d)$ and $R^{min}(d)$ for the case when phase shifts δ_{14}, δ_{24} and δ_{34} coincide and equal $\pi/2$, while Fig. 3, *b* presents the dependences obtained at $\delta_{14} = \delta_{24} = \pi/2$ and $\delta_{34} = -\pi/2$. As the plots show, the maximum possible reflection coefficient ($R^{max} = 1.6 \cdot 10^{-2}$) gets achieved when FWM takes place on three secondary gratings 14, 24 and 34 with phase shifts of $\pi/2$. In this case, the highest value of R^{max} is 50% higher than R^{max} obtained for gratings 14, 24 (Fig. 2, *a*) and 25% higher than the highest R achievable for gratings 14, 34 at $\delta_{14} = \delta_{34} = \pi/2$. Variation in the phase shift of grating 34 from $\pi/2$ to $-\pi/2$ significantly affects the intensity of the phase-conjugated wave. When condition $\delta_{14} = \delta_{24} = \delta_{34} = \pi/2$ was met, the value of the reflection coefficient exceeded diffraction efficiency η at the crystal thickness below 5.6 mm for any value of azimuth ψ (Fig. 3, *a*).

When $\delta_{34} = -\pi/2$, the opposite situation is observed: coherent subtraction of the diffraction contributions of gratings 14, 24 and grating 34 leads to the fact that parameter η exceeds R^{max} for any azimuth ψ at the crystal thickness below 5.6 mm. If the crystal thickness is greater than 5.6 mm, an excess of the reflection coefficient over

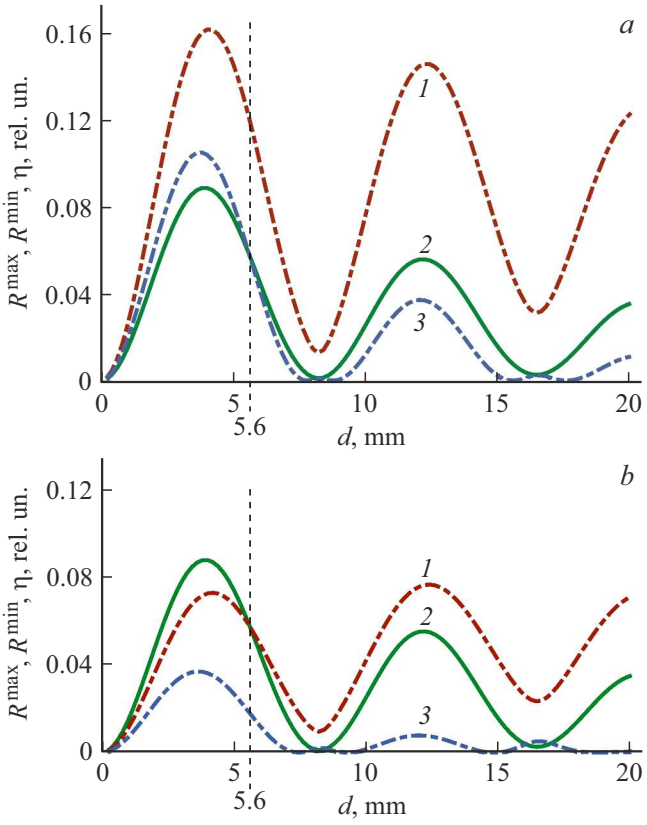

Figure 3. Reflection hologram diffraction efficiency η (curve *2*) and reflection coefficients R^{max} (curve *1*), R^{min} (curve *3*) during FWM versus crystal thickness d. Dependences $R^{max}(d)$, $R^{min}(d)$ were calculated for the cases when gratings 14, 24 and 34 are formed during FWM with the following phase shifts: *a* — $\delta_{12} = \delta_{24} = \delta_{34} = \pi/2$; *b* — $\delta_{12} = \delta_{24} = \pi/2$, $\delta_{34} = -\pi/2$.

diffraction efficiency can be provided in both cases under consideration by selecting the optimal value of azimuth ψ. At the local minima of the $R^{\max}(d)$ dependences taking place when conditions $\rho d = \pi/2,\ 3\pi/2$ are met, parameter $R^{\max}$ has approximately equal values in Figs. 3, *a* and *b*.

Thus, the numerical solution of the coupled-wave equations proposed in [8] makes it possible to predict the holographic experiment conditions (initial azimuths of the light wave linear polarization, crystal thickness) under which the highest phase-conjugate wave intensities get achieved during forward FWM on shifted gratings in a cubic optically active photorefractive absorbing crystal. It is shown that selection of the optimal conditions for the FWM experiment can provide a 50% increase in the reflection coefficient in the (001)-cut BSO crystal.

Financial support

The study was supported by the Belarus Republic Ministry of Education (Contract № 1410/2021 of 22.03.2021) in the framework of State Research Program № 6 „Photonics and electronics for innovations“ for 2021–2025 (Assignment 6.1.14).

Conflict of interests

The author declares that he has no conflict of interests.

References

[1] N.V. Nikonorov, V.M. Petrov, Opt. Spectrosc., **129**, 530 (2021). DOI: 10.1134/S0030400X21040172.
[2] V.M. Petrov, A.V. Shamray, *Interferentsiya i difraktsiya dlya informatsionnoy fotoniki* (Lan, SPb, 2019). (in Russian)
[3] A. Blazquez-Castro, A. García-Cabanes, M. Carrascosa, Appl. Phys. Rev., **5**, 041101 (2018). DOI: 10.1063/1.5044472
[4] M.P. Petrov, S.I. Stepanov, A.V. Khomenko, *Fotorefraktivnye kristally v kogerentnoy optike* (Nauka, SPb, 1992). (in Russian)
[5] Y. Ding, H.J. Eichler, Opt. Commun., **110**, 456 (1994). DOI: 10.1016/0030-4018(94)90449-9.
[6] S.G. Odulov, M.S. Soskin, A.I. Khizhnyak, *Lazery na dinamicheskikh reshetkakh: opticheskie generatory na chetyrekhvolnovom smeshchenii* (Nauka, M., 1990). (in Russian)
[7] V.N. Naunyka, Opt. Spectrosc., **130** (3), 324 (2022). DOI: 10.21883/EOS.2022.03.53557.2936-21.
[8] V.N. Naunyka, Bull. Lebedev Phys. Inst., **49** (Suppl. 1), S58 (2022). DOI: 10.3103/S1068335622130073.
[9] V.N. Naunyka, A.V. Makarevich, Phys. Solid State, **65** (3), 441 (2023). DOI: 10.21883/PSS.2023.03.55587.516.
[10] S.M. Shandarov, N.I. Burimov, Yu.N. Kul'chin, R.V. Romashko, A.L. Tolstik, V.V. Shepelevich, Quantum Electron., **38** (11), 1059 (2008). DOI: 10.1070/QE2008v038n11ABEH013793.

Translated by Solonitsyna Anna